Supplementary Information

Copper nanoparticles-embedded hydrogel for killing bacteria and promoting wound healing with photothermal therapy

Bailong Tao[a], Chuanchuan Lin[a], Yiman Deng[a], Zhang Yuan[a], Xinkun Shen[a], Maowen Chen[a], Ye He[a], Zhihong Peng[b], Yan Hu[a], Kaiyong Cai[a,c]*

[a] Key Laboratory of Biorheological Science and Technology, Ministry of Education College of Bioengineering, Chongqing University, Chongqing 400044, China

[b] Department of Gastroenterology, Southwest Hospital, Third Military Medical University (Army Medical University), Chongqing 400038, China

[c] Chongqing Key Laboratory of Soft-Matter Material Chemistry and Function Manufacturing, Chongqing, 400044, China

* Corresponding author: Prof. Dr. Kaiyong Cai

College of Bioengineering

Chongqing University,

Chongqing 400044,

China

Tel: +86-23-65111802

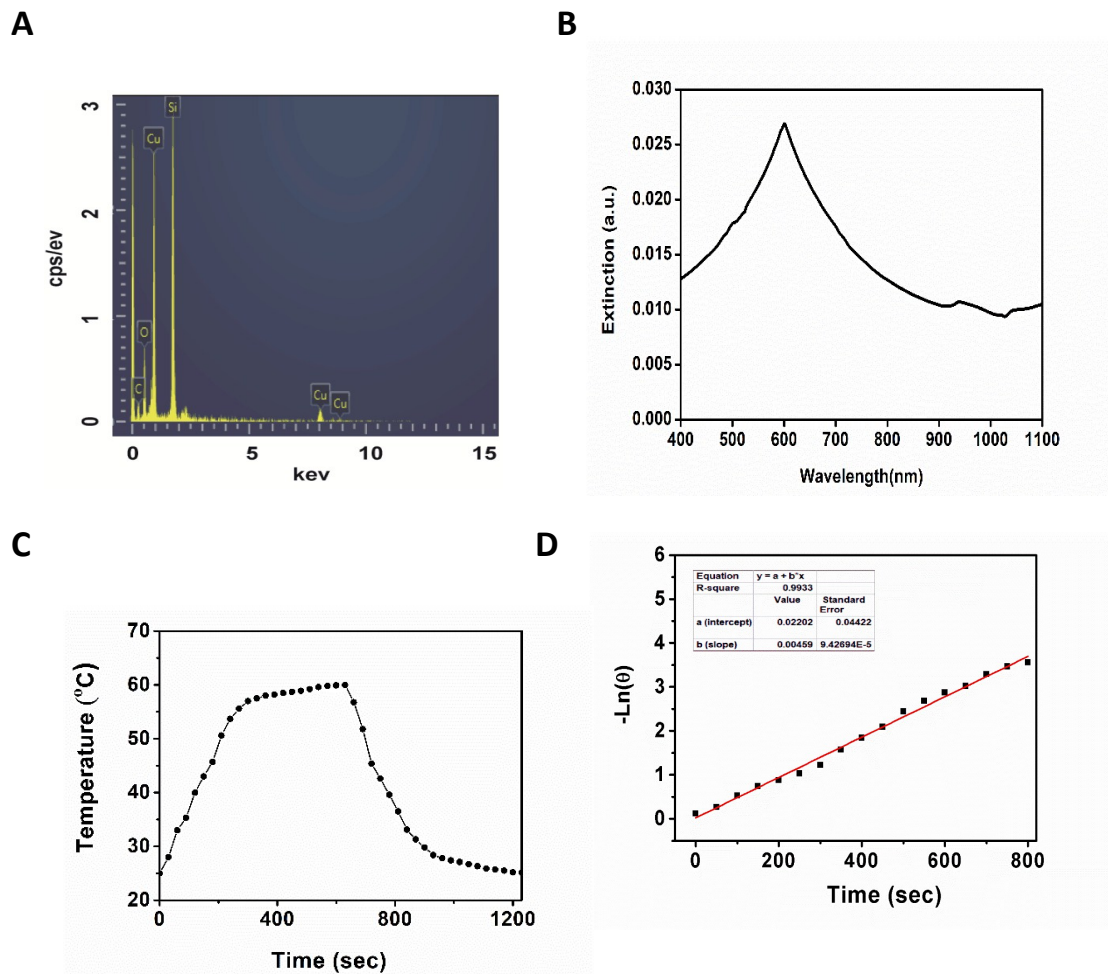Fax: +86-23-65102877

E-mail: kaiyong_cai@cqu.edu.cn

Figure S1. Characterization of Cu nanoparticles: (A) EDS spectrum and (B) normalized UV-vis absorption spectrum of the prepared Cu nanoparticles. (C) Temperature increase and cooling period of Cu nanoparticles embedded hydrogel irradiated at 808 nm NIR-laser (1.2 W/cm²) over one on/off cycle. (D) Linear time data versus –Ln (θ) collected from the cooling period (after 800 s) *vs* negative natural logarithm of driving force temperature of Figure S1. Time constant for heat transfer from the Cu nanoparticles- embedding hydrogel was determined to be τ_S =216.43 s.
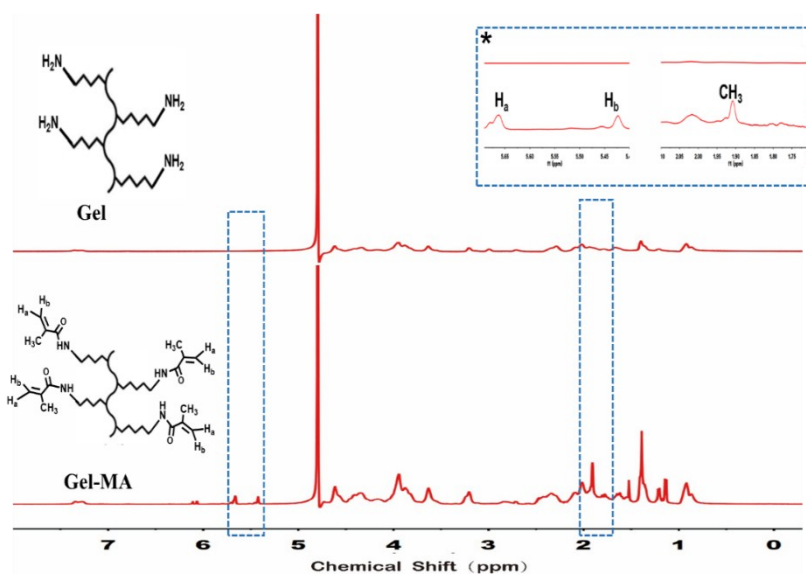
Figure S2. ^{1}HNMR spectra of gelatin (Gel) and gelatin methacrylamide (Gel-MA) forms prepared in D2O at room temperature. The expanded region in Gel-MA between 5.40 and 5.65 ppm as well as methyl presented in 1.91 ppm (shown with an asterix) is presented as inset, showing the methacrylation of gelatin.

To verify that the methacryloyl group was introduced to gelatin, ^{1}HNMR measurement was employed. Compared with bare gelatin, Gel-MA showed three additional peaks (methylene, δ=5.40 and 5.65 ppm and methyl peak, δ=1.91 ppm) attributing to the introduction of methacrylic anhydride into gelatin. Furthermore, the degree of methacrylation of gelatin was also counted with the peaks of 5.40 and 5.65 ppm for the double bonds of the methacrylate groups and 7.40 ppm for the aromatic amino acid residues of gelatin.[S1] Thus, we confirmed that the photo-active Gel-MA was successfully obtained and the methacrylation of gelatin corresponded to approximately 52% by the quantitative ^{1}HNMR analysis.[S1, S2]
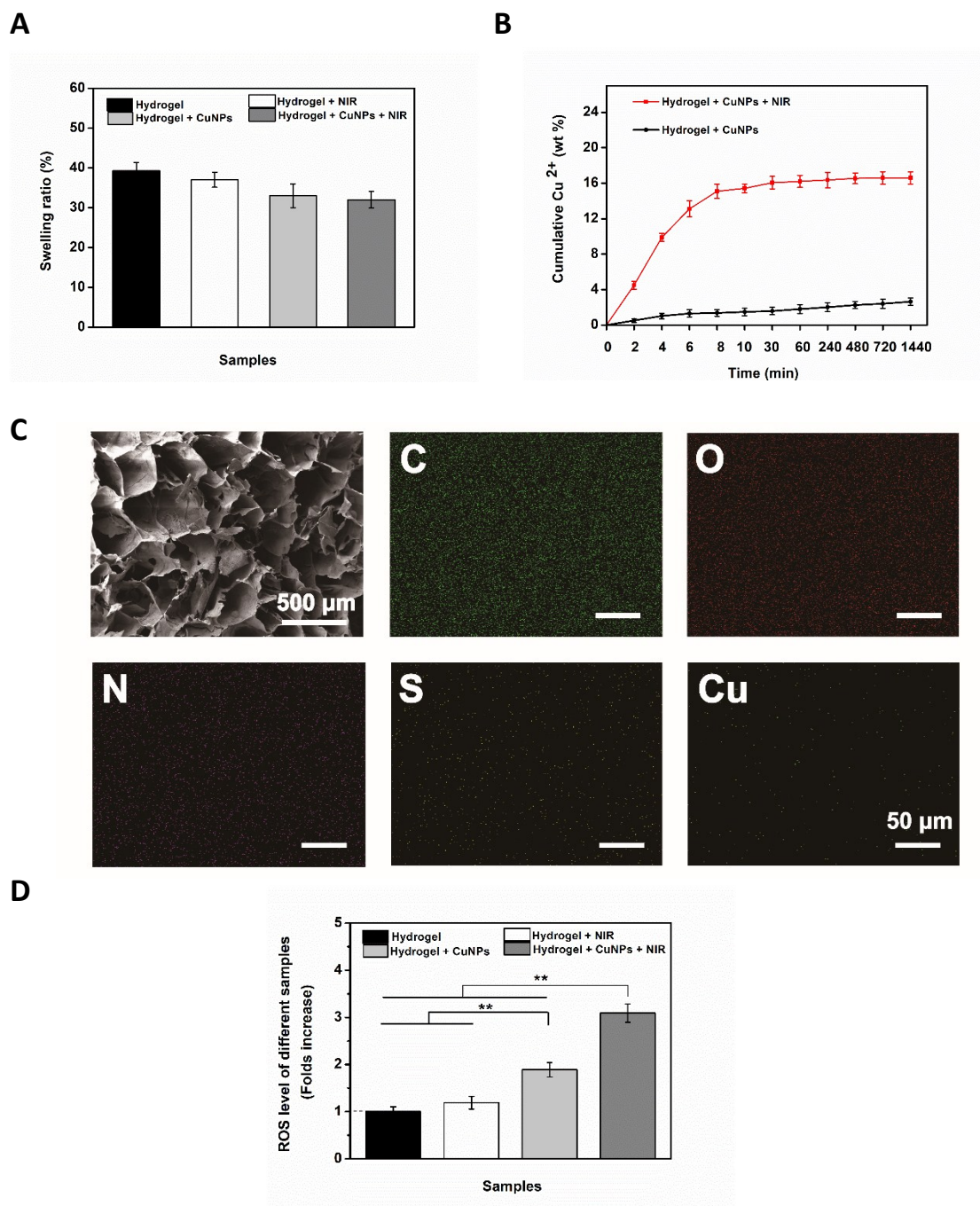
Figure S3. (A) Swelling ratios (in PBS, pH = 7.4) of hydrogel samples at 37°C for 24 h.

(B) The release profiles of Cu NPs from hybrid hydrogels with or without 808nm laser

irradiation at different time intervals (n = 3). (C) SEM image and corresponding

elements of C, O, N, S and Cu. (D) ROS levels of various samples normalization to

hydrogel group. Error bars represent mean ± SD for n = 6, **p < 0.01.
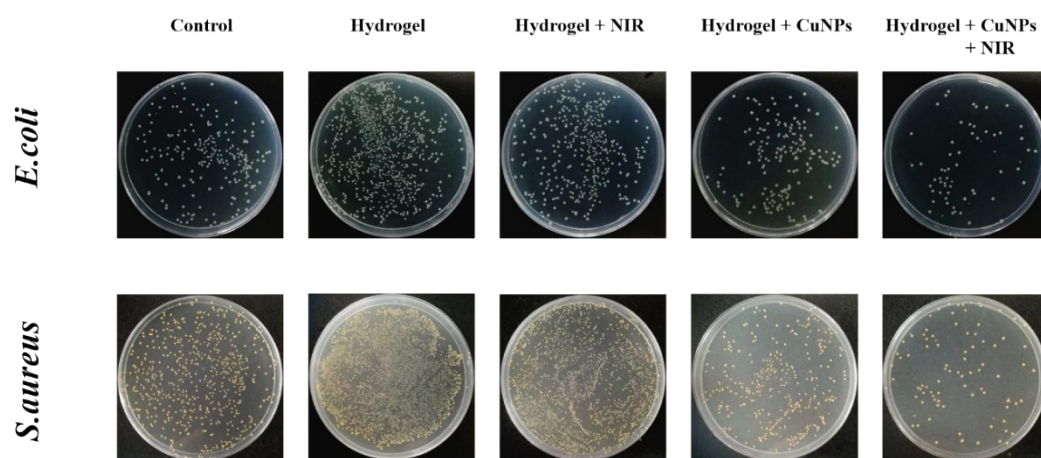
Figure S4. Photographs of formed viable colony units of *E. coli* (up) and *S. aureus* (bottom) after treatments with different samples when exposing to the 808 nm laser irradiation for 10 min or not. Bacterial cells were then spread onto LB agar plate and incubated at 37 °C for further 24 h.
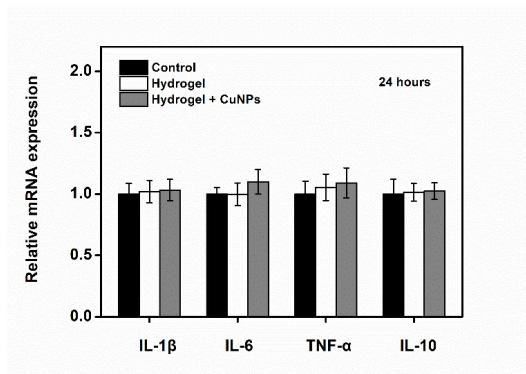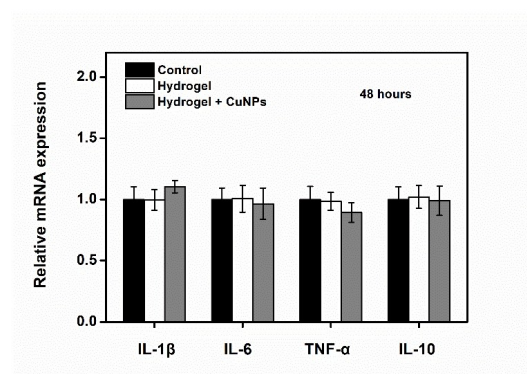
A　　　　　　　　　　　　　　**B**

Figure S5. Real-time PCR analysis of inflammation-related gene expression (IL-1β, IL-6, TNF- α, and IL-10) by Raw264.7 in control, hydrogel and hydrogel + Cu NPs at 24 (A) and 48 h (B). Error bars represent mean ± SD for n = 3.
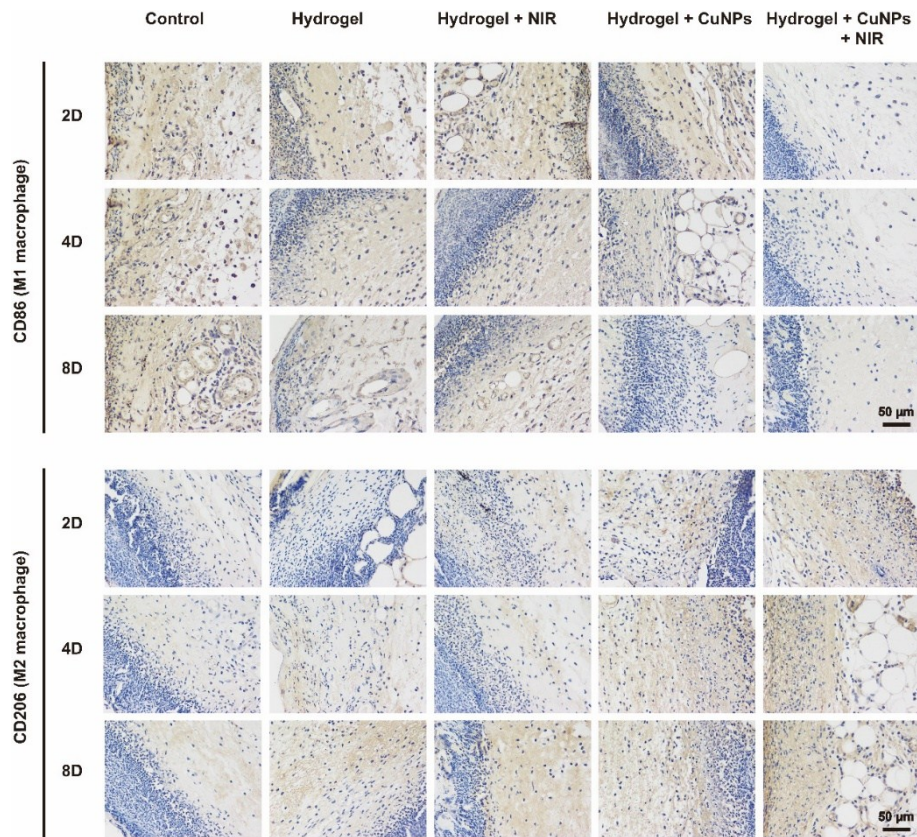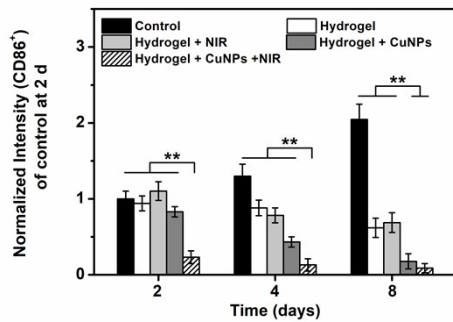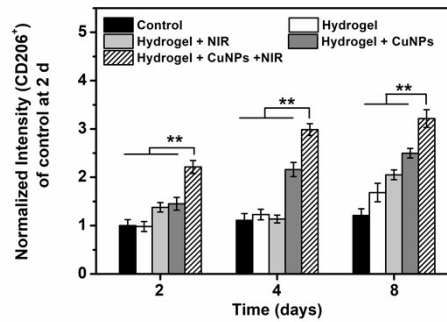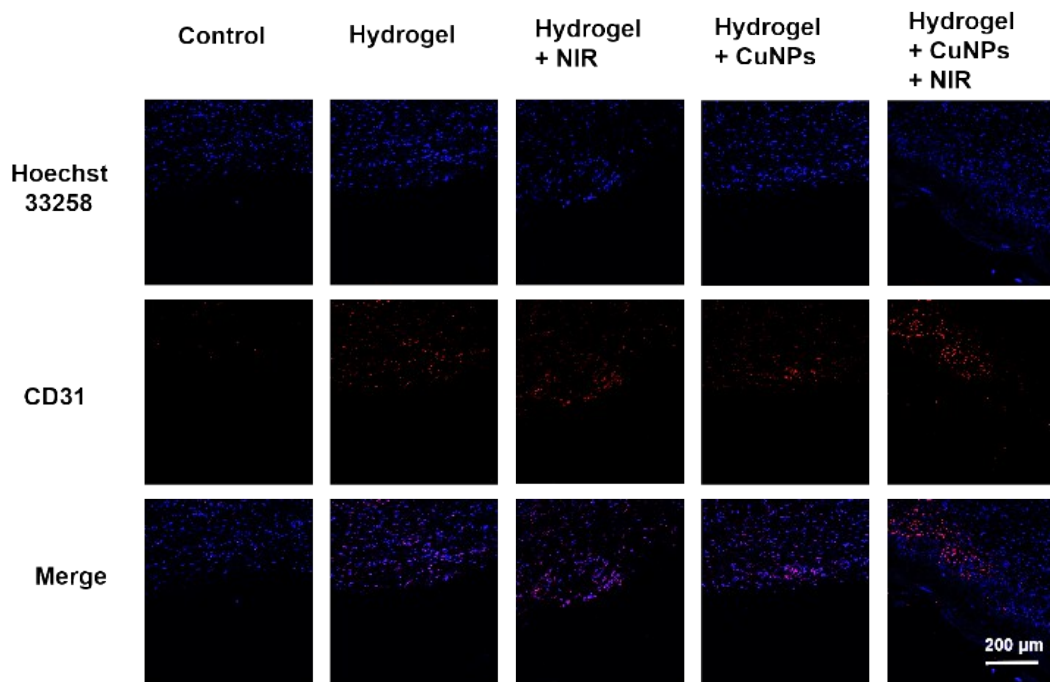
A

B **C**

Figure S6. (A) Representative immunohistochemistry images of CD86 (M1 macrophage) and CD206 (M2 macrophage) of wound sites during wound healing for inflammatory responses evaluation in different groups on day 2, 4 and 8 post-injury. The relevant quantitative analysis of CD 86 (B) and CD 206 (C) intensity. Error bars represent mean ± SD for n = 3, **p < 0.01.
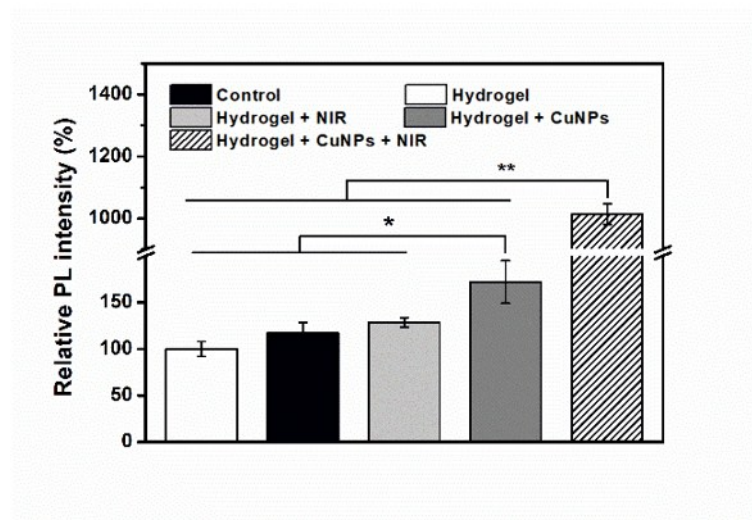
A

B

Figure S7. (A) Angiogenesis after treatment for 14 days stained for nuclei (blue) and CD31 (red), respectively. (B) Quantitative analysis of CD31-positive blood vessel formation based on the immunohistochemistry images (n = 3), *p < 0.05, **p < 0.01.
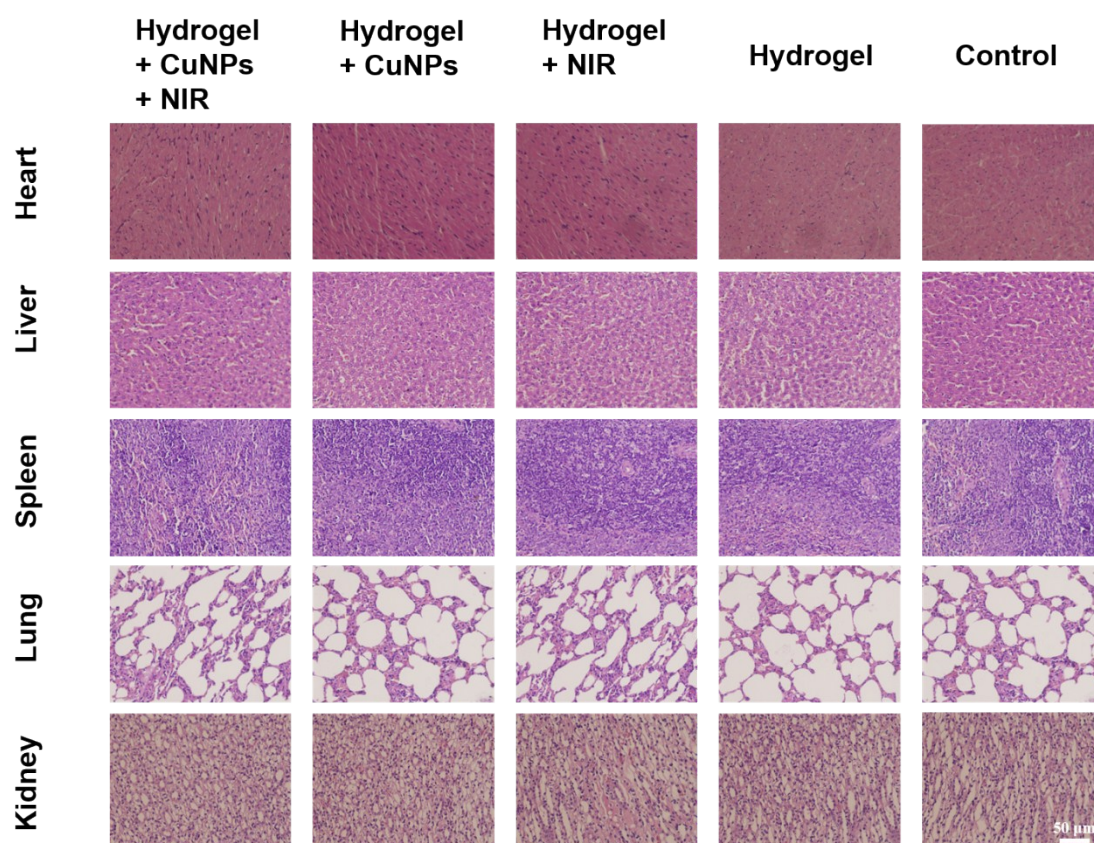
Figure S8. H&E staining of the major organs of SD mice heart, liver, spleen, lung, and kidney for toxicological observation after 14 days of treatment in different groups.

Table S1. Primers used for qRT-PCR in this study.

Genes	Accession no.	Primers	Product size (bp)
IL-1β	NM_008361.4	5'- TGCCACCTTTTGACAGTGATG-3' 5'- TGATGTGCTGCTGCGAGATT -3'	135
IL-6	NM_012589.2	5'- CACTTCACAAGTCGGAGGCT-3' 5'- TCTGACAGTGCATCATCGCT -3'	114
TNF-α	NM_013693.3	5'- CAGGCGGTGCCTATGTCTC-3' 5'-CGATCACCCCGAAGTTCAGTA-3'	89
IL-10	NM_012854.2	5'- TTGAACCACCCGGCATCTAC-3' 5'- CCAAGGAGTTGCTCCCGTTA-3'	114
β-Actin	NM_031144.3	5'-GGCTCCTAGCACCATGAAGAT-3' 5'-AAGGGTGTAAAACGCAGCTC-3'	202

References

[S1] J. W. Nichol, S. T. Koshy, H. Bae, C. M. Hwang, S. Yamanlar and A. Khademhosseini, *Biomaterials*, 2010, **31**, 5536-5544.

[S2] X. Yi, J. P. He, X. L. Wang, Y. Zhang, G. X. Tan, Z. N. Zhou, J. Q. Chen, D. F. Chen, R. X. Wang, W. Tian, P. Yu, L. Zhou and C. Y. Ning, *ACS Appl. Mater. Interfaces*, 2018, **10**, 6190–6198.